Competition between Coqblin-Schrieffer and local exchange interactions in Kondo systems by the perturbative renormalization group

Eva Pavarini
Max-Planck Institut für Festkörperforschung, D-70569 Stuttgart, Germany
and Institut de Physique Théorique, Université de Lausanne, BSP, CH-1015 Lausanne, Switzerland

Lucio Claudio Andreani
Istituto Nazionale per la Fisica della Materia, Dipartimento di Fisica ''A. Volta,'' Università di Pavia, I-27100 Pavia, Italy
(Received 17 September 1998)

A model which accounts for the competition between hybridization and local exchange (LE) interactions in anomalous Ce systems is proposed. In this model a localized magnetic moment $j_f=5/2$ has an antiferromagnetic Coqblin-Schrieffer (CS) coupling with $l=3$ conduction electrons partial waves, due to hybridization, and a contact coupling with $l=0$ partial waves due to the LE interaction. The last term breaks the SU(N) symmetry of the CS model. Using the perturbative renormalization group, we show that the SU(N) ground state of the CS model remains the ground state even in the presence of a LE interaction stronger than the CS coupling. We discuss the effect of the LE on the Kondo temperature. Moreover, when the LE coupling reaches a critical value the system has a non-Fermi-liquid non-SU(N) ground state, and when it is stronger than the critical value the system falls into an undercompensated Kondo state. [S0163-1829(99)00210-6]

I. INTRODUCTION

In normal rare earth systems, intra-atomic correlations tend to form a stable $4f^n$ configuration. The local exchange (LE) interaction produces a ferromagnetic (FM) coupling ($J_{sf}>0$) between the spin density of $l=0$ conduction electron partial waves at the rare earth ion site $\mathbf{s}(0)$, and the spin of the rare earth ion in the Hund's rule ground multiplet $\mathbf{S}_f$. This coupling results in an exchange interaction between $\mathbf{s}(0)$ and $\mathbf{J}_f$, the Hund's rule ground multiplet total angular momentum, with coupling constant $(g_J-1)J_{sf}$, where g_J is the Landé factor. Since the local spin coupling J_{sf} is ferromagnetic, the coupling constant is antiferromagnetic (AFM) for the first half of the rare earth series, and FM for the second half. In addition, the LE interaction produces an indirect magnetic coupling of the Ruderman-Kittel-Kasuya-Yosida (RKKY) type between the magnetic moment of the rare earth ions, which is responsible for the onset of magnetic order.[1]

In diluted Ce and Yb systems, the hybridization induces local spin fluctuations within the ground state configuration of the impurity $4f^n$ ($4f^1$ for Ce and $4f^{13}$ for Yb), via virtual mixing with the excited $4f^{n\pm1}$ configurations, producing a quenching of the localized magnetic moment at low temperature. The simplest model which describes the anomalous phenomena related to hybridization and, at the same time, accounts for the orbital degrees of freedom of the f impurity, is the degenerate Anderson model,[2] which can be mapped onto the CS model in the spin fluctuation limit.[3,4] The CS model, in which a localized magnetic moment moment $\mathbf{J}_f$ has an AFM contact interaction $J_{\rm hyb}<0$ with $l=3$ conduction electron partial waves, acts on the lowest Hund's rule multiplet of the ground configuration. The CS Hamiltonian gives results in good agreement with experimental data on dilute compounds, and is widely used to understand the Kondo related anomalies in Ce and Yb systems.[5]

In dense Ce and Yb systems, the Kondo effect, which favors a nonmagnetic heavy Fermi-liquid ground state, competes with the indirect pair coupling, which originates from both LE and hybridization and tends to produce a magnetic ground state. The presence of Kondo anomalies is often taken as an evidence that hybridization dominates over LE. However, electronic structure calculations suggest that in anomalous Ce compounds such as CeTe, CeSe, and CeAg the magnetic interaction is determined by LE rather than by the hybridization-induced pair coupling.[6] The explanation of this apparent paradox is one of the main purpose of this paper.

Recently we have shown,[7] using a spin 1/2 two band model including competing ferromagnetic and antiferromagnetic exchange interaction, that the Kondo effect may persist at low temperature even in the presence of a strong local exchange. However, those conclusions come from a model in which the degeneracy of the f shell is neglected. In this paper we study a realistic model in which the orbital degeneracy is included, and both hybridization and local exchange are retained. The model in the form given here applies to Ce and Yb systems; detailed results will be given for the case of cerium.

The CS model is invariant under SU(N) transformations in the angular momentum space. This symmetry, which is higher than spherical, has to be a result of approximations in the starting Hamiltonian, namely the degenerate Anderson model. SU(N) symmetry is broken by the presence, i.e., of interactions which split the excited f-impurity configurations.[8,9] As shown by Hirst, the coupling between f and conduction electrons is more general than the usual CS coupling if we consider the realistic atomic level structure in the excited configurations.[9] Studying a generalized [i.e., non-SU(N)] CS model, we have shown that this kind of symmetry breaking scales to weak coupling,[8] and therefore the presence of multiplet splittings does not alter the low-

temperature physics of the model. However, the LE interaction also induces a breaking of the SU(N) symmetry of the CS model. Therefore, in this paper we also study the stability of the SU(N) symmetry with respect to the presence of LE interaction.

This paper is organized as follows. In Sec. II we describe the model Hamiltonian and the tensor operator approach adopted. In Sec. III we describe the method used, namely, the perturbative renormalization group, and derive the scaling equations. In Sec. IV we illustrate the results of the scaling procedure in some relevant cases. In Sec. V the implications of the results are briefly discussed.

II. MODEL

The CS Hamiltonian[3] may be written as

$$H_{\rm CS}=\sum_k \sum_{m=-j_f}^{j_f} \epsilon_k \hat{n}_{km} - J_{\rm hyb} \sum_{kk'} \sum_{m,m'=-j_f}^{j_f} \times \left[c^\dagger_{k'm'} c_{km} c^\dagger_{fm} c_{fm'} - \frac{\delta_{m,m'}}{N_f} c^\dagger_{k'm'} c_{km} \right]. \quad (1)$$

Here ϵ_k is the energy of $l=3$ conduction electrons with wave vector $\mathbf{k}$, $J_{\rm hyb}$ is the AFM coupling constant generated from hybridization through the Schrieffer-Wolff canonical transformation,[3,4] j_f is the total angular momentum of the impurity in the Hund's rules ground multiplet ($j_f=5/2$ for the $4f^1$ configuration and $j_f=7/2$ for the $4f^{13}$ configuration) and $N_f=2j_f+1$ is the f ground multiplet degeneracy. The operator c_{km} annihilates a conduction electron in a spin-orbit eigenstate made of $l=3$ partial waves.

The LE Hamiltonian, projected onto the Hund's rules ground multiplet space, may be written as

$$H_{\rm LE}=\sum_\nu \sum_{\sigma=-1/2}^{\sigma=1/2} \epsilon_\nu \hat{n}_{\nu\sigma} - (g_J-1) J_{sf}\, \mathbf{s}(0)\cdot \mathbf{J}_f, \quad (2)$$

where ϵ_ν is the energy of $l=0$ conduction electrons with wave vector ν. $J_{sf}>0$ is the FM coupling constant, the Landé factor is $g_J=6/7$ for Ce and $g_J=8/7$ for Yb and $s(0)$ is the spin density of $l=0$ electrons at the impurity site.

The two Hamiltonians $H_{\rm CS}$ and $H_{\rm LE}$ may be rewritten using multipolar tensor operators for f and conduction electrons defined as[9,8]

$$T^n_q(j_f)=\sum_{m,m'=-j_f}^{j_f} \sqrt{2n+1}(-1)^{j_f-m'} \times \begin{pmatrix} j_f & n & j_f \\ -m' & q & m \end{pmatrix} c^\dagger_{fm'} c_{fm}, \quad (3)$$

$$t^n_q(j_c)=\sum_{kk'} \sum_{m,m'=-j_c}^{j_c} \sqrt{2n+1}(-1)^{j_c-m'} \times \begin{pmatrix} j_c & n & j_c \\ -m' & q & m \end{pmatrix} c^\dagger_{k'm'} c_{km}. \quad (4)$$

The symbols $\begin{pmatrix} j & n & j \\ -m' & q & m \end{pmatrix}$ are the $3j$ symbols,[10] j_f (j_c) is the f (conduction) electron total angular momentum, $T_q{}^n$ ($t_q{}^n$) is the f (conduction) electron tensor operator of order n, and component $q=-n,\ldots,n$. The rank of the tensors, n, assumes all integer values from $n=0$ to $N_m=\min\{N_f,N_c\}-1$, where $N_c=2j_c+1$. The operators T^n_q and t^n_q are orthonormal, since

$$\mathrm{Tr}_c[t^n_q(j_c)(t^{n'}_{q'})^\dagger(j_c)]=\mathrm{Tr}_f[T^n_q(j_f)(T^{n'}_{q'})^\dagger(j_f)]=\delta_{nn'}\delta_{q,q'}. \quad (5)$$

The scalar product between two tensor operators is defined in the following way:

$$\mathbf{T}^n(j_f)\cdot\mathbf{t}^n(j_c)=\sum_q (-1)^q T^n_q(j_f) t^n_{-q}(j_c). \quad (6)$$

The generalized Hamiltonian considered in this paper is written as follows:

$$H=\sum_k \sum_{m=-j_f}^{m=j_f} \epsilon_k n_{km} + \sum_{n=0}^{2j_f} a_n \mathbf{T}_n\cdot\mathbf{t}_n + \sum_\nu \sum_{\sigma=-1/2}^{\sigma=1/2} \epsilon_\nu n_{\nu\sigma} + b_1 \mathbf{T}_1\cdot\mathbf{p}_1. \quad (7)$$

The first term in Hamiltonian (7) describes the band energy of the $l=3$ partial waves. The second one describes the contact coupling between the f multiplet and the total magnetic moment density of the $l=3$ partial waves at the impurity site. Since the angular momentum indices of the localized state and $l=3$ conduction electron partial waves are the same, the rank of both tensor $\mathbf{T}_n(j_f)$ and $\mathbf{t}_n(j_f)$ assumes all integer values from $n=0$ to $N_m=N_f-1$. We have renamed, for simplicity, $\mathbf{T}_n(j_f)\to\mathbf{T}_n$, $\mathbf{t}_n(j_f)\to\mathbf{t}_n$. The sum of the first and second terms in Eq. (7) gives a ''generalized CS'' Hamiltonian, where the SU(N) symmetry can be broken. The third term in Eq. (7) describes the band energy of $l=0$ partial waves. The last term describes the contact coupling between $\mathbf{J}_f$ and the spin density of $l=0$ partial waves at the impurity site. Since $j_c=1/2$ for this band, and therefore $N_m=1$, only the tensors of rank 1, $\mathbf{T}_1(j_f)$, and $\mathbf{t}_1(1/2)$, are present. We have renamed, for simplicity, $\mathbf{t}_1(1/2)\to\mathbf{p}_1$. The sum of the last two terms in Eq. (7) gives a Kondo Hamiltonian, which describes the compensated Kondo problem if $j_f=1/2$, and the undercompensated problem if $j_f>1/2$.

The Hamiltonian (7) with generic a_n and b_1 is obviously more general than $H_{\rm CS+LE}=H_{\rm CS}+H_{\rm LE}$, since the CS part does not have SU(N) symmetry. A particular model $H_{\rm model}$ may be written in the form (7) using the orthogonality property of tensor operators

$$a_n=\mathrm{Tr}_f\,\mathrm{Tr}_c\, T^n_0 t^n_0 H_{\rm model}, \quad (8)$$

$$b_1=\mathrm{Tr}_f\mathrm{Tr}_c T^1_0 p^1_0 H_{\rm model}. \quad (9)$$

We analyze the case of $H_{\rm model}=H_{\rm CS+LE}$. The CS model $H_{\rm CS}$ contributes only to the first two terms in Eq. (7). We find $a_n=-J_{\rm hyb}$, and therefore $a_n>0$ (AFM); both tensors $\mathbf{T}_n$ and $\mathbf{t}_n$, with $n=0,1,\ldots,N_f-1$, act in a space of dimension N_f. The LE interaction $H_{\rm LE}$ contributes only to the last

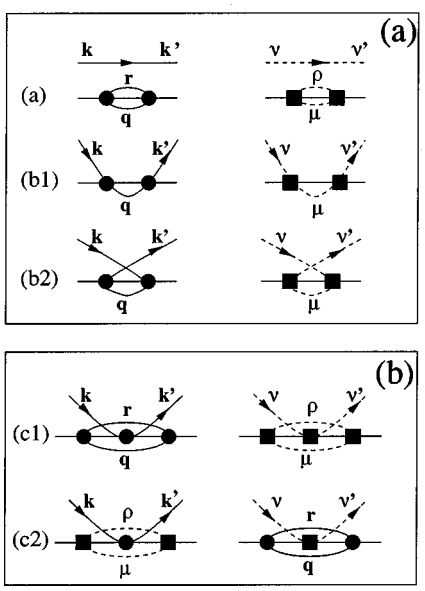

FIG. 1. (a) Two-vertex diagrams which contribute to the scaling equations. The diagrams are explained in the text. (b) Three-vertex diagrams which contribute to the scaling equations. The diagrams are explained in the text.

two terms in Eq. (7). We find $b_1=-(g_J-1)J_{sf}\sqrt{\mathrm{Tr}_f\, J_z^2\, \mathrm{Tr}_c\, j_z^2}$, with $\mathrm{Tr}_c\, j_z^2=1/2$, and therefore, for Ce systems, $b_1=\sqrt{5/28}J_{sf}>0$ (AFM); $\mathbf{T}_1$ acts in a space of dimension N_f, while $\mathbf{p}_1$ acts in a space of dimension $N_c=2$. Therefore, in the case of Ce systems, the generalized Hamiltonian (7) has six independent parameters: a_n, $n=1,\ldots,5$, and b_1.

In Ref. 7 we considered a two band model in which a localized spin 1/2 has a FM exchange interaction with one band (which stands for $l=0$ partial waves) and an AFM exchange coupling with the other one (which corresponds to $l=3$ partial waves). This model may be rewritten in the form of the Hamiltonian (7) if we take $j_f=1/2$. For this spin 1/2 two band model, only two parameters are different from zero, $a_1=-J_{\mathrm{hyb}}/2>0$ (AFM) and $b_1=-J_{sf}/2<0$ (FM).

III. SCALING EQUATIONS

We adopt the perturbative scaling method introduced by Anderson.[11] This method is based on the idea that, as the band cutoff is reduced, an increasing number of states can be eliminated from the conduction band, provided that the original interaction between the f impurity and the conduction electrons is transformed into a renormalized effective one. Following this procedure, we therefore reduce the band cutoff B (we assume for simplicity that the band cutoff is the same for $l=3$ and $l=0$ partial waves) to $B-|\delta B|$, and find the transformed Hamiltonian $H'=H-\delta H$, with $\delta H=\sum_{n=0}^{N_m}\delta a_n \mathbf{T}_n\cdot\mathbf{t}_n+\delta b_1\mathbf{T}_1\cdot\mathbf{p}_1$. We have calculated δa_n and δb_1 up to third order in the coupling constants, since it is known that, in the cases of the Kondo and CS models, it is just at this order that both the proper low-temperature behavior and the correct expression for the Kondo temperature are recovered.[5].

In Fig. 1 we show diagrammatically the scattering processes which contribute up to third order to the scaling equations. Diagrams should be read in the following way: circles (squares) are CS (LE) interaction vertices, lines running from left to right (right to left) are propagators of electron (hole) states. Lines above the horizontal line connecting vertices correspond to electrons (holes) with energy ϵ, $E_F<\epsilon<B-|\delta B|$ $(-B+|\delta B|<\epsilon<E_F)$, where E_F is the Fermi level. Lines below are electrons or holes at the band edges. Solid **k**, **r**, and **q** lines are $l=3$ electron (hole) states with energy ϵ_k, ϵ_r, and ϵ_q, respectively. Dashed ν, ρ, and μ lines are $l=0$ electron (hole) states with energy ϵ_ν, ϵ_ρ, and ϵ_μ. The propagators of the intermediate states (**q**, **r**, μ, and ρ lines) are integrated over the intermediate states moments.

The connected two-vertex diagrams (b1) and (b2) in Fig. 1(a) contribute to the scaling equation at the second order, while the connected three-vertex diagrams (c1) and (c2) in Fig.1(b) contribute at the third order. Disconnected two-vertex diagrams (a) in Fig. 1(a), give rise to a wave function renormalization factor, and therefore contribute to the scaling equations only at the third order.[5]

We find a system of N_f coupled scaling equation (we set for simplicity the band density of states $\rho=1$ for both $l=3$ and $l=0$ partial waves)

$$\delta a_n=\left[\sum_{n'n''}\mathcal{M}^n_{n'n''}a_{n'}a_{n''}+a_n\sum_{n'}\mathcal{N}^n_{n'}a^2_{n'}+a_n b_1^2\mathcal{N}^n_1\right]\delta\ln B, \tag{10}$$

$$\delta b_1=\left[-\frac{b_1^2}{\sqrt{\mathrm{Tr}_f\, J_z^2\, \mathrm{Tr}_c j_z^2}}+\frac{b_1^3}{\mathrm{Tr}_f\, J_z^2}+b_1\sum_{n'}\mathcal{N}^1_{n'}a^2_{n'}\right]\delta\ln B, \tag{11}$$

where

$$\mathcal{M}^n_{n'n''}=(2n'+1)(2n''+1)\begin{Bmatrix} n & n' & n'' \\ j_f & j_f & j_f\end{Bmatrix}^2 \times[(-1)^{n+n'+n''}-1](-1)^{2j_f+2j_c}, \tag{12}$$

$$\mathcal{N}^n_{n'}=(2n'+1)\left[\begin{Bmatrix} n' & j_f & j_f \\ n & j_f & j_f\end{Bmatrix}(-1)^{n+n'}+\frac{(-1)^{N_f}}{N_f}\right](-1)^{N_f}, \tag{13}$$

and

$$\mathcal{N}^n_1=\frac{(2n+1)(n+1)n}{6\ \mathrm{Tr}_f\, J_z^2}=\frac{2n+1}{3}\mathcal{N}^1_n. \tag{14}$$

The quantities $\{\begin{smallmatrix} j_1 & j_2 & j_3 \\ j_4 & j_5 & j_6\end{smallmatrix}\}$ are the $6j$ symbols.[10]

If $j_f=1/2$, the system (10), (11) reduces to the two scaling equations already discussed in Ref. 7 for the spin 1/2 two-band model. In the rest of the paper we will focus the attention on the case of $4f^1$ ground state configuration, even if the Hamiltonian (7) and the scaling equations above have a more general validity. Therefore, the Hamiltonian has six independent parameters, and the full space of the scaling trajectories has dimension 6.

TABLE I. The fixed points found in this work. Here $C=\mathrm{Tr}_f J_z^2/\mathrm{Tr}_c j_z^2$. The terminology generalizes that used in Ref. 8, where (A1) was called (a), (B1) (b), (C1) (c), (D1) (d), (E1) (e), and (F1) (f). Going to all orders in the scaling equations, the strong coupling fixed points (A2) and (C1) will be moved to ($a=0, b_1 \to \infty$) and ($a \to \infty, b_1=0$), respectively.

Fixed point	a_1	a_2	a_3	a_4	a_5	b_1
(A1)	0	0	0	0	0	0
(A2)	0	0	0	0	0	$\sqrt{C}$
(B1)	1	0	0	0	0	0
(B2)	$C/(C+1)$	0	0	0	0	$\sqrt{C}/(C+1)$
(C1)	1	1	1	1	1	0
(D1)	1	0	1	0	1	0
(E1)	1	-1	1	-1	1	0
(F1)	1	0	0.3883	0	-2.0087	0
(G1)	0.69	0.54	0.38	0.25	0.16	1.74

IV. RESULTS

The general system of scaling equations (10), (11) is quite complicated when the full six-dimensional space of parameters is considered. Therefore we have focused our attention on four physically relevant sets of starting points. The various fixed points found in this work are summarized in Table I, where the terminology generalizes that used in Ref. 8. We note that the fixed point (A1), $a_1=a_2=a_3=a_4=a_5=b_1=0$, is the trivial, unstable, weak coupling fixed point. This fixed point can be reached from all subspaces of starting points we will consider below.

(i) *Generalized Coqblin-Schrieffer model*. The first set of starting points [set (i)] considered in this work is defined by the condition ($b_1=0$, $a_n \neq 0$). This set describes models in which the LE interaction is neglected (hybridization only problem), and includes, e.g., the SU(N) symmetric CS model itself. In this subspace, the Hamiltonian (7) reduces to the generalized CS Hamiltonian.[8] The space of the trajectories we are dealing with has dimension 5.

All the scaling trajectories starting from the subspace ($b_1=0$, $a_n \neq 0$) remain in this subspace during the scaling flow. Depending on the starting point, a trajectory may end in one of the following fixed points. (A1), which is the unstable weak coupling fixed point. (B1) $b_1=0, a_1=1, a_2=0, a_3=0, a_4=0, a_5=0$, which is the fixed point of the compensated dipolar Kondo effect. (C1) $a_1=1, a_2=1, a_3=1, a_4=1, a_5=1, b_1=0$. This is the strong coupling fixed point of the CS model. (D1) $b_1=0, a_2=a_4=0, a_1=a_3=a_5=1$, (E1) $b_1=0, a_2=a_4=-1, a_1=a_3=a_5=1$, (F1) $b_1=0, a_2=a_4=0, a_1=1, a_5=-2.0087, a_3=0.3883$. The physically most relevant of those fixed points is (C1), which is the strong coupling fixed point of the SU(N) symmetric CS model. We have already studied in detail this subspace and the stability of its fixed points in Ref. 8.

In Ref. 8 we have shown that all the trajectories starting from the AFM quadrant ($a_n>0$) always lead to the fixed point (C1). Numerically, we have seen that the trajectories starting from the AFM quadrant lead to the fixed point (C1) even in the presence of a small LE term (i.e., $b_1=\Delta b_1$, and $|\Delta b_1| \ll 1$, $|\Delta b_1| \ll |a_n|$). Therefore, the main result obtained in Ref. 8 for the generalized CS model does not change qualitatively due to the presence of a small LE term: the SU(N) symmetry breaking interactions described in the generalized CS model continue to scale to weak coupling. Actually, a small LE deviation from a point in subspace (i), e.g., the point $a_n=\tilde{a}_n$, $b_1=0$, scales to weak coupling, as we can see if we set $b_1=\Delta b_1$ with $|\Delta b_1| \ll 1$, $a_n=\tilde{a}_n+\Delta a_n$ with $|\Delta a_n| \ll 1$ (here $|\Delta a_n| \sim |\Delta b_1|$), and derive the linearized scaling equation for b_1, namely ,

$$\delta \Delta b_1 \sim \Delta b_1 \sum_n \mathcal{N}_n^1 \tilde{a}_n^2 \delta \ln B. \tag{15}$$

Since $\mathcal{N}_n^1>0, \Delta b_1$ decreases in absolute value when the cutoff is decreased.

These conclusions are valid if the LE term is small, i.e., if $|\Delta b_1| \ll 1$, $|\Delta b_1| \ll |a_n|$. However, as we will see below [see cases (iii) and (iv)] a finite LE term may change strongly the ground state properties of the model.

(ii) *Local exchange only*. The second set considered [set (ii)] is defined by the condition $b_1 \neq 0$, $a_1=a_2=a_3=a_4=a_5=0$. This condition reduces the six-dimensional space to a line, the line $a_n=0 \forall n$, along which we found two fixed points (A1) and (A2). We have already discussed the weak coupling fixed point (A1). (A2) is the stable strong coupling fixed point $a_1=0, a_2=0, a_3=0, a_4=0, a_5=0, b_1=\sqrt{C}$, where $C=\mathrm{Tr}_f J_z^2/\mathrm{Tr}_c j_z^2$. For example, in the case $j_f=5/2$, $C=35$, and (A2) is the strong coupling fixed point of the undercompensated Kondo model.[12] In the case $j_f=1/2$, we find $C=1$ and (A2) is the strong coupling fixed point of the compensated Kondo problem. The trajectories starting from $a_n=0$, $b_1>0$ end in (C1), while the trajectories starting from $a_n=0$, $b_1<0$ end in (A2): thus when the dipolar coupling is antiferromagnetic ($b_1>0$) and $j_f>1/2$, the undercompensated Kondo effect takes place.

(iii) *Coqblin-Schrieffer + local exchange*. The third set we consider [set (iii)] is the SU(N) symmetric set, defined by the conditions $b_1 \neq 0$, $a_n=a \neq 0$: this condition reduces the six-dimensional space of the scaling trajectories to a plane, the plane ($a_n=a, b_1$). The model Hamiltonian $H_{\mathrm{CS+LE}}$ is a starting point of type (iii), as we have seen above. In the plane defined by the set (iii), all the three fixed points (A1), (A2), and (C1) are present. It is interesting to study the stability of (A2) and (C1) in the whole six-dimensional space, and the competition between the fixed points (C1) and (A2) when the starting parameters are varied.

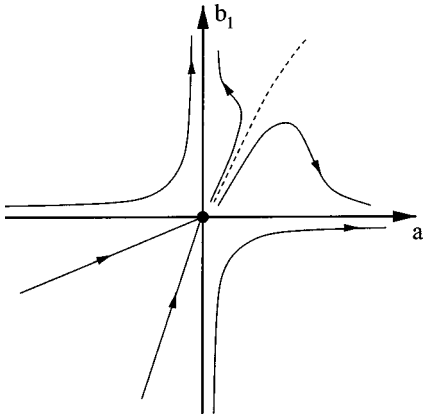

FIG. 2. Sketch of the scaling trajectories for the case (iii) $a_n = a, b_1$, $j_f = 5/2$.

The fixed point (A2) is stable in the whole six-dimensional space, as we have seen numerically and by linearizing the scaling equations around (A2). If we set $a_n = \Delta a_n$, where $|\Delta a_n| \ll 1$, and $b_1 = \Delta b_1 + \sqrt{C}$, where $|\Delta b_1| \ll 1$, the linearized scaling equations are

$$\Delta a_n \sim C \Delta a_n \mathcal{N}_1^n \delta \ln B, \tag{16}$$

$$\Delta b_1 \sim \frac{\Delta b_1}{\mathrm{Tr}_c\, j_z^2} \delta \ln B. \tag{17}$$

Since $\mathcal{N}_1^n > 0$ and $\mathrm{Tr}_c\, j_z^2 > 0$, the fixed point is stable along each direction.

The fixed point (C1) is also stable in the whole six-dimensional space. If we set $a_n = \Delta a_n + \delta_{n,1}$, where $|\Delta a_n| \ll 1$, and $b_1 = \Delta b_1$, where $|\Delta b_1| \ll 1$, the linearized scaling equations are

$$\delta \Delta a_n \sim N_f \Delta a_n \delta \ln B, \tag{18}$$

$$\delta \Delta b_1 \sim N_f \Delta b_1 \delta \ln B, \tag{19}$$

and therefore a small deviation from the fixed point decreases in absolute value as the cutoff is decreased.

The scaling equations are valid only for $|a| \ll 1, b_1 \ll 1$: for the full solution of the model (i.e., if we go beyond perturbative regime) the strong coupling fixed points (A2) and (C1) will be moved, respectively to $a = 0, b_1 \to \infty$ and $a \to \infty$, $b_1 = 0$, as for the Kondo and the CS models.[13]

Only trajectories starting from the axes (i.e., from $b_1 = 0, a \neq 0$ or from $b_1 \neq 0, a = 0$) remain in the plane during the scaling flow: SU(N) symmetry is generally broken during the scaling. However, most of the trajectories starting from set (iv) end in the starting plane. In Fig. 2 the projection of those trajectories onto the SU(N) symmetric plane is shown. We have found that the trajectories starting from $b_1 > 0, a > 0$, end in (A2) when $b_1 > \beta a$ and in (C1) when $b_1 < \beta a$, with $\beta \sim 10$. The trajectories which fall on the line $b_1 \sim \beta a$ (the dashed line in Fig. 2) leave the plane and fall into a NFL fixed point (G1) obtained numerically as $b_1 = 1.74$, $a_1 = 0.69$, $a_2 = 0.54$, $a_3 = 0.38$, $a_4 = 0.25$, $a_5 = 0.16$. The trajectories starting from FM values $b_1 > 0, a < 0$ end in (A2), and starting from values $b_1 < 0, a > 0$ end in (C1). The trajectories starting from values $b_1 < 0, a < 0$ end in the weak coupling fixed point (A1).

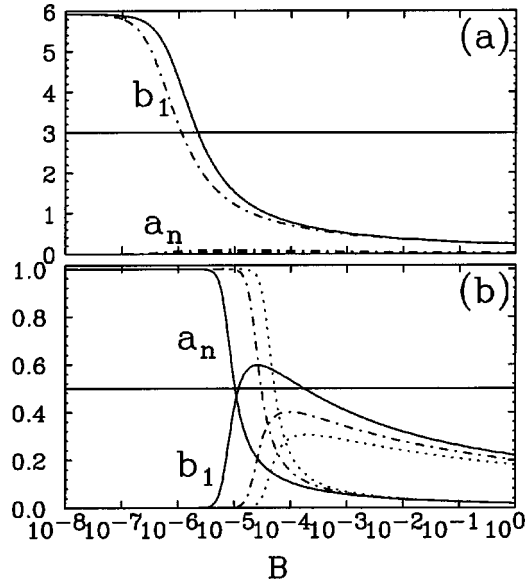

FIG. 3. Variation of parameters upon scaling, as a function of the band cutoff for $j_f = 5/2$. (a) The starting point are chosen in the undercompensated Kondo regime. Solid line: starting point $a = 0, b_1 = 0.24$. Dash-dotted lines: starting point $a = 0.02, b_1 = 0.24$. The parameters a_n, hardly distinguishable from the horizontal axis, scale to weak coupling. The parameter b_1 scales to strong coupling. (b) The starting points are chosen in the CS regime. From left to right: starting point $a = 0.02, b_1 = 0.22$ (solid lines), starting point $a = 0.02, b_1 = 0.20$ (dot-dashed lines), starting point $a = 0.02, b_1 = 0.18$ (dotted lines). The parameters a_n scales to strong coupling, while b_1 scales to weak coupling.

The two physical interactions in Hamiltonian $H_{\mathrm{CS+LE}}$ are both AFM, corresponding to starting points of the type $b_1 > 0, a > 0$. We have found two physical regimes for this Hamiltonian: in the first one the system falls into an undercompensated Kondo ground state as the temperature approaches zero ($b_1 > \beta a$) and in the second one the system falls into a CS model ground state ($b_1 < \beta a$). Since $\beta \sim 10$, this means that, for the case of Ce compounds ($j_f = 5/2$), the borderline between the two regimes is reached when $J_{sf}/|J_{\mathrm{hyb}}| \sim 25$. Therefore, the compensated CS state is the ground state even if $|J_{\mathrm{hyb}}|$ is 25 times smaller than J_{sf}.

For the usual CS model (i.e., $b_1 = 0, a_n = a > 0$), the characteristic temperature T_0 may be derived from the third order scaling equations, by defining it as the value reached by the band cutoff B when the coupling constant becomes equal to a given value, e.g., one half the value at the fixed point. It can be shown that

$$T_0^{\mathrm{CS}} = B (N_f a)^{1/N_f} \exp(-1/N_f a), \tag{20}$$

in agreement with the exact expression.[5] The same is true for the Kondo model (i.e., $b_1 = b > 0, a_n = 0$), with

$$T_0^K = B \left(\frac{b}{\sqrt{\mathrm{Tr}_f\, J_z^2\, \mathrm{Tr}_c\, j_z^2}} \right)^{\mathrm{Tr}_c j_z^2} \exp\left(- \frac{\sqrt{\mathrm{Tr}_f\, J_z^2\, \mathrm{Tr}_c\, j_z^2}}{b} \right). \tag{21}$$

Since $\mathrm{Tr}_c j_z^2 = 1/2$, the expression in Eq. (21) reduces to the usual formula $T_0^K = B\sqrt{|J|}\exp(1/J)$, where $J = -\sqrt{2}b/\sqrt{\mathrm{Tr}_f\, J_z^2}$. For the model H_{LE}, $J=(g_J-1)J_{\mathrm{sf}}$, and $J<0$ (AFM) for Ce systems, the case considered in this work. Therefore, in the CS regime, we define the characteristic temperature for our model in the same way, as the value reached by B when $a_n \sim 0.5$. In the Kondo regime, T_K is the value reached by B when $b_1 \sim 3$.

In Fig. 3(a) we show the variation of the parameters upon scaling as a function of the band cutoff for starting points in the undercompensated Kondo regime. In particular, we show the cases $b_1=0.24$, $a=0$ (solid line) and $b_1=0.24$, $a=0.02$ (dot-dashed line). The Kondo temperature of the model is the value of B for which $b_1(B)=3$ [crossing between the horizontal solid line and $b_1(B)$]. We see that, when a increases, the Kondo temperature of the model is reduced.

In Fig. 3(b) we show the variation of the parameters upon scaling as a function of the band cutoff for starting points in the CS regime. We show (from left to right) the cases $a=0.02$, $b_1=0.22$ (solid line), $a=0.02$, $b_1=0.20$ (dot-dashed line), and $a=0.02$, $b_1=0.18$ (dotted line). The Kondo temperature of the model is the value of B for which $a(B)=0.5$ [crossing between the horizontal solid line and $a(B)$]. We see that, as b_1 increases and therefore the ratio b_1/a approaches the critical value, the characteristic temperature of the generalized CS model [Fig. 3(b)] approaches the Kondo temperature of the undercompensated Kondo model [Fig. 3(a)]: the transition takes place when the two characteristic temperatures are equal. Since, apart from the prefactors, $T_0^{\mathrm{CS}} \sim B\exp(-1/6a)$ if $b_1=0$, and $T_0^K \sim B\exp(-\sqrt{35}/2b_1)$ if $a=0$, we expect the transition to be around $b_1 \sim 18a$. The critical ratio b_1/a is overestimated, because we have neglected the prefactors and the fact that both T_0^{CS} and T_0^{K} change when both a_n and b are different from zero [see Figs. 3(a) and 3(b)].

(iv) *Dipolar coupling + local exchange*. The last set of starting points we consider [set (iv)] is the one defined by the condition $a_1 \neq 0, a_2=a_3=a_4=a_5=0, b_1 \neq 0$. Again, we have reduced the six-dimensional trajectories space to a plane. This set is interesting because it describes, e.g., a dipolar Kondo coupling plus a local exchange interaction, which is the generalization of the two band (or two-channel) model studied in Ref. 7 to the case in which the localized moment is $j_f \geqslant 1/2$. In the plane (a_1, b_1) there are four fixed points, (A1), which is the unstable weak coupling fixed point discussed above, (A2), which is the fixed point of the undercompensated Kondo effect, stable in the whole space, as we have seen before, (B1) which is the fixed point of the compensated dipolar Kondo effect. It is stable in the plane but not in the whole space, as we have seen numerically and by linearizing the scaling equations around it. (B2) $b_1=\sqrt{C}/(1+C)$, $a_1=C/(1+C)$, $a_2=0, a_3=0, a_4=0, a_5=0$, which is stable only along the line $a_1=\sqrt{C}b_1$. This fixed point is the generalization of the non-Fermi-liquid (NFL) fixed point found by Pang and Cox[14] for the two-channel Kondo model. The two channel Kondo model is recovered when $j_f=1/2$ and, in that case, $C=1$. For the full solution of the model (i.e., if we go beyond the perturbative regime) the strong coupling fixed points (A2) and (B2) will be moved to $a \to \infty$, $b_1=0$ and $a_1=0, b_1 \to \infty$, respectively.[13]

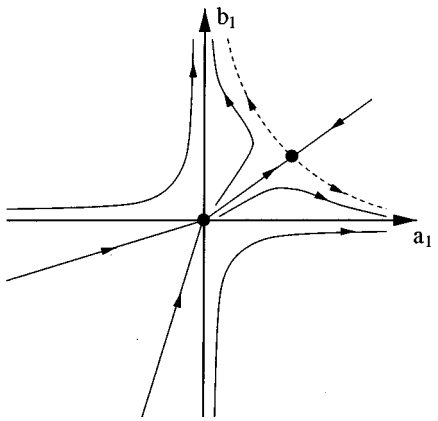

FIG. 4. Sketch of the scaling trajectories for the case (iv) $a_1 \neq 0$, $b_1 \neq 0$, $a_2=a_3=a_4=a_5=0$, and $j_f=5/2$.

All the trajectories of type (iv) remain of type (iv) during the scaling. Therefore, the scaling equations reduce to

$$\delta a_1 = \left[-\frac{a_1^2}{\mathrm{Tr}_f\, J_z^2} + \frac{a_1^3 + a_1 b_1^2}{\mathrm{Tr}_f\, J_z^2} \right] \delta \ln B, \tag{22}$$

$$\delta b_1 = \left[-\frac{b_1^2}{\sqrt{\mathrm{Tr}_f\, J_z^2\, \mathrm{Tr}_c\, j_z^2}} + \frac{b_1^3 + b_1 a_1^2}{\mathrm{Tr}_f\, J_z^2} \right] \delta \ln B. \tag{23}$$

For $j_f=1/2$, the scaling equations coincide with those found in Ref. 7.

In Fig. 4 we show the trajectories projected onto the plane (a_1, b_1), which are quite similar to those of case (iii), except for the fact that the NFL fixed point now lies in the plane. The trajectories starting from the FM quadrant $a_1<0, b_1<0$ end in (A1). The trajectories starting from $a_1<0, b_1>0$ end in (A2). The trajectories starting from $a_1>0, b_1<0$ end in (B1). The trajectories starting from the AFM quadrant may end in (A2), (B1), (B2). They end in (A2) if $a_1<\sqrt{C}b_1$, in (B1) if $a_1>\sqrt{C}b_1$, and in (B2) if $a_1=\sqrt{C}b_1$. We have therefore three regimes for the AFM model: the compensated dipolar Kondo regime for $a_1>\sqrt{C}b_1$, the NFL regime for $a_1=\sqrt{C}b_1$, and the undercompensated Kondo state for $a_1<\sqrt{C}b_1$. In the compensated Kondo regime, the characteristic temperature of the model is the value of B for which $a_1(B)=0.5$. When $b_1=0$, $T_0^c = B\sqrt{(2a_1/C)}\exp(-C/2a_1)$. As b_1 increases, the characteristic temperature decreases. In the undercompensated Kondo regime, the characteristic temperature of the model is the value of B for which $b_1(B)=\sqrt{C}/2$. When $b_1=0$, $T_0^u = B\sqrt{(2b_1/\sqrt{C})}\exp(-\sqrt{C}/2b_1)$. As a_1 increases, the characteristic temperature decreases. When the ratio a_1/b_1 approaches the critical ratio $(a_1/b_1=\sqrt{C})$, the characteristic scale of the compensated model approaches that of the undercompensated model. The crossover between the two regimes is given by the condition $a_1/b_1=\sqrt{C}$, when the two characteristic temperatures are equal.

For $j_f=1/2$ the fixed point (A2) describes the compensated Kondo ground state; in this case the scaling trajectories shown in Fig. 4 coincide with those calculated in Ref. 7. In particular, when the two interactions have opposite signs, the

ground state is always determined by the AFM interaction and is the compensated Kondo state.

V. DISCUSSION AND CONCLUSIONS

We have proposed and studied a model to describe the competition between hybridization and LE in anomalous Ce systems, accounting for the effects of the orbital degrees of freedom of the *f* electrons. In this model, a localized *f* impurity has a generalized CS coupling with $l=3$ conduction electron partial waves and a LE interaction with $l=0$ partial waves. The LE interaction breaks the SU(N) symmetry in angular momentum space of the CS model. The present model is also the starting point for studying the role of crystal-field effects on the competition between hybridization and local exchange.

We have shown that the SU(N) symmetry breaking scales to weak coupling when the ratio $J_{sf}/|J_{\rm hyb}|$ is lower than a critical value of the order of 25. In this regime the system falls, at low temperature, into the ground state of the SU(N) CS model. However, due to the presence of LE, the characteristic temperature of the model is lower than the Kondo temperature of the CS model alone. Moreover, when $J_{sf}/|J_{\rm hyb}|\sim 25$, the system falls into a non-Fermi-liquid non-SU(N) ground state. Finally, when $J_{sf}/|J_{\rm hyb}|>25$, the system has an undercompensated Kondo state.

In Ref. 8 we have already shown that the SU(N) symmetry breaking interactions described by a generalized CS model (e.g., virtual mixing with the realistic atomic levels in the excited configurations) scale to weak coupling. Here, we have shown that SU(N) symmetry is stable even in the presence of a LE coupling, provided that $J_{sf}<25|J_{\rm hyb}|$. Those results justify the success of the CS model in explaining the low temperature physics of anomalous Ce and Yb systems.

In a dense system, the Kondo effect competes with the pair coupling between localized moments $I_{\rm RKKY}$ which is generated by both hybridization and local exchange. A study of this competition at mean-field level shows that the system is magnetic when the coupling $I_{\rm RKKY}$ is larger than T_K.[15,16] When $J_{sf}/|J_{\rm hyb}|\ll 1$, the system will be nonmagnetic with a heavy Fermi-liquid ground state if the pair coupling is lower than the Kondo temperature. Let us imagine now that the LE coupling increases and becomes stronger than hybridization ($J_{sf}/|J_{\rm hyb}|>1$): the system can still have a Kondo-like ground state if both conditions $J_{sf}/|J_{\rm hyb}|<25$ and $I_{\rm RKKY}<T_K$ are satisfied. When $J_{sf}/|J_{\rm hyb}|=25$ or $J_{sf}/|J_{\rm hyb}|>25$ the system will have a NFL or an undercompensated Kondo ground state, respectively, if the Kondo temperature is still larger than the pair coupling. However, in the presence of a very strong LE coupling, the pair coupling will dominate over the Kondo effect, and therefore the system will become magnetic and the effects related to hybridization will be suppressed. Since the CS ground state is realized even for relatively large ratios $J_{sf}/|J_{\rm hyb}|$, it is fully possible that for large values of $J_{sf}/|J_{\rm hyb}|$ (but <25) the magnetic interaction is dominated by the local exchange contribution: thus the present results provide an explanation for the dominance of LE in the magnetic interaction, even in systems such as CeS, CeSe, CeAg, where a Kondo phenomenology with reduction of the ordered moments is established.

ACKNOWLEDGMENTS

The authors are indebted to G. Amoretti and P. Santini for several helpful discussions, and to A.C. Hewson for useful correspondence. O. Jepsen is acknowledged for the careful reading of the mauscript.

[1] J. Jensen and A. R. Mackintosh, *Rare Earth Magnetism* (Clarendon, Oxford, 1991).
[2] P.W. Anderson, Phys. Rev. **124**, 41 (1961).
[3] B. Coqblin and J.R. Schrieffer, Phys. Rev. **185**, 847 (1969).
[4] J.R. Schrieffer and P.A. Wolff, Phys. Rev. **149**, 491 (1966).
[5] A. C. Hewson, *The Kondo Problem to Heavy Fermions* (Cambridge University Press, Cambridge, England, 1993).
[6] N. Kioussis, B.R. Cooper, and J.M. Willis, Phys. Rev. B **44**, 10 003 (1991); Q.G. Sheng and B.R. Cooper, *ibid.* **50**, 965 (1994); P. Monachesi, L.C. Andreani, A. Continenza, and A.K. McMahan, J. Appl. Phys. **73**, 6634 (1993).
[7] E. Pavarini and L.C. Andreani, Phys. Rev. Lett. **77**, 2762 (1996).
[8] E. Pavarini and L.C. Andreani, Phys. Rev. B **56**, 5073 (1997).
[9] L.L. Hirst, Adv. Phys. **27**, 231 (1978).
[10] A. R. Edmonds, *Angular Momentum in Quantum Mechanics* (Princeton University Press, Princeton, NJ, 1957).
[11] P.W. Anderson, J. Phys. C **3**, 2436 (1970).
[12] P. Schlottman and P.D. Sacramento, Adv. Phys. **42**, 641 (1993).
[13] P. Nozières and A. Blandin, J. Phys. (France) **41**, 193 (1980).
[14] H.B. Pang and D.L. Cox, Phys. Rev. B **44**, 9454 (1991).
[15] D.L. Cox, Phys. Rev. B **35**, 4561 (1987).
[16] L.C. Andreani, E. Liviotti, P. Santini, and G. Amoretti, Z. Phys. B **100**, 95 (1996).